Inorg. Chem. **1983**, *22*, 3267-3275

Contribution from the Department of Chemistry,
University of Minnesota, Minneapolis, Minnesota 55455

Rhodium and Iridium Complexes of 2-(Bis(diphenylphosphino)methyl)pyridine (PNP). X-ray Crystal and Molecular Structures of $[Rh_2(CO)_2(PNP)_2](PF_6)_2 \cdot C_3H_6O$ and $[Ir_2(\mu\text{-}CO)(CO)_2(PNP)_2](BF_4)_2$ and Some Chemistry of These and Related Complexes

MICHAEL P. ANDERSON, C. C. TSO, BRUCE M. MATTSON,† and LOUIS H. PIGNOLET*

Received February 8, 1983

Binuclear diphosphine-bridged complexes with the tridentate ligand 2-(bis(diphenylphosphino)methyl)pyridine, $(Ph_2P)_2CHC_5NH_4$ = PNP, have been prepared for rhodium and iridium. Two of the complexes, $[Rh_2(CO)_2(PNP)_2](PF_6)_2 \cdot C_3H_6O$ (**1**) and $[Ir_2(\mu\text{-}CO)(CO)_2(PNP)_2](BF_4)_2$ (**2**), have been characterized by single-crystal X-ray diffraction. Complex **1** crystallizes in the orthorhombic space group *Pbcn* with $Z = 4$, $a = 19.658$ (7) Å, $b = 18.528$ (7) Å, $c = 17.993$ (6) Å, $V = 6554$ (7) Å^3, and $d = 1.553$ g/cm^3 while **2** crystallizes in the triclinic space group $P\bar{1}$ with $Z = 4$, $a = 16.387$ (4) Å, $b = 16.710$ (6) Å, $c = 24.710$ (6) Å, $\alpha = 76.03$ (2)°, $\beta = 84.16$ (2)°, $\gamma = 75.37$ (2)°, $V = 6347$ (4) Å^3, and $d = 1.638$ g/cm^3. Both complexes are of the diphosphine-bridged binuclear type with trans phosphorus atoms and with both pyridyl nitrogen atoms bonded to the metal atoms, giving five-membered PN chelate rings. The pyridyl nitrogen atoms are bonded to the metals on the same side of the binuclear complex. Complex **1** is of the face-to-face variety with a Rh···Rh separation of 3.054 (1) Å while **2** has a bridging CO ligand and approximate trigonal-bipyramidal geometry around each iridium atom. The Ir–Ir separation in **2** is 2.815 (1) Å and is consistent with the presence of an Ir–Ir bond. Complex **2** easily loses one CO ligand in solution, affording the iridium analogue of **1**. Reactions of these complexes with nucleophiles such as halide and sulfide ions are described. Thus, **1** reacts with Cl^- in acetone solution, giving the four-coordinate PN-bonded monomeric compound [Rh(Cl)(CO)(PNP)], which has a dangling phosphorus atom, whereas the analogous reaction with **2** gives the binuclear complex $[Ir_2(Cl)(CO)_2(PNP)_2]^+$, which has one bonded and one free pyridyl nitrogen atom. The reaction of **1** with S^{2-} gives the binuclear sulfide-bridged A-frame complex $[Rh_2(\mu\text{-}S)(CO)_2(PNP)_2]$, which has both pyridyl nitrogen atoms dangling. All of these complexes have been characterized by IR and ^{31}P NMR spectroscopy, and their syntheses and properties are described.

Introduction

Binuclear complexes using bis(diphenylphosphino)methane (dppm) and 2-(diphenylphosphino)pyridine (Ph_2Ppy)[1] ligands to hold two metal atoms in close proximity have received considerable attention in recent years.[1-10] The dppm ligand has been found to bridge metal atoms with various coordination numbers and in a number of different geometries. Typical of these binuclear structural types are the face-to-face dimers, A, the molecular A-frames, B, and the double A-frames, C.

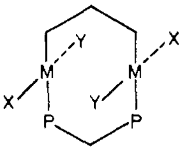

A

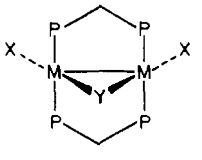

B

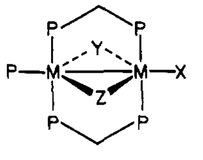

C

The Ph_2Ppy ligand has not been as extensively studied as dppm, but it also is beginning to show an interesting binuclear chemistry.[1,11] As a result of the proximity of the two metals in these complexes, a number of interesting chemical reactions have been observed. These include metal–metal bond forming and bond breaking and the insertion of small molecules into the M–M bond.[4,12,13]

An unusual example of a M–M bond-forming reaction is the addition of CO to molecules of type A, giving a M–M-bonded dimer with a bridging CO ligand. Such a reaction has been observed: $[Rh_2(t\text{-}BuNC)_4(dppm)_2]^{2+} + CO \rightarrow [Rh_2(\mu\text{-}CO)(t\text{-}BuNC)_4(dppm)_2]^{2+}$.[9] A more common method for preparing bridged A-frame type complexes from A (M = Rh, X = halide, Y = CO) involves loss of halide or CO, giving, for example $[Rh_2(\mu\text{-}Cl)(CO)_2(dppm)_2]^+$[5,6,14] or $[Rh_2(\mu\text{-}CO)Br_2(dppm)_2]$.[3b] There are very few dicationic binuclear complexes of types A–C, and the *t*-BuNC complex above represents a rare example.

We have started to examine binuclear complexes with the potentially tridentate ligand 2-(bis(diphenylphosphino)methyl)pyridine, $(Ph_2P)_2CHC_5H_4N$ = PNP. This ligand offers a choice of PP or PN bidentate or PNP tridentate coordination with four- and/or five-membered chelate rings. Binuclear complexes of Rh(I) and Ir(I) are also likely to be dicationic since the pyridyl N atom may function as a neutral ligating group. In the past this ligand has attracted relatively little attention.[15,16] However, we have recently reported on the synthesis of metal complexes where PNP is tridentate to one Rh atom and where it bridges two Rh atoms via its phosphorus atoms, forming binuclear complexes similar to types A and B.[15] Details of some of this work and results with analogous iridium complexes are reported here. These studies include some novel M–M bond-forming reactions of type A complexes by the addition of bridging ligands.

Experimental Section

Physical Measurements. $^{31}P\{^1H\}$ NMR spectra were recorded at

---

† On leave from the Department of Chemistry, Creighton University, Omaha, NE 68178.

(1) Farr, J. P.; Olmstead, M. M.; Hunt, C. H.; Balch, A. L. *Inorg. Chem.* **1981**, *20*, 1182.
(2) Kubiak, C. P.; Woodcock, C.; Eisenberg, R. *Inorg. Chem.* **1982**, *21*, 2119.
(3) (a) Cowie, M.; Dwight, S. K. *Inorg. Chem.* **1980**, *19*, 2500. (b) *Ibid.* **1980**, *19*, 2508.
(4) Kubiak, C. P.; Eisenberg, R. *Inorg. Chem.* **1980**, *19*, 2726 and references cited therein.
(5) Cowie, M.; Dwight, S. K. *Inorg. Chem.* **1979**, *18*, 2700.
(6) Cowie, M. *Inorg. Chem.* **1979**, *18*, 286.
(7) Holloway, R. G.; Penfold, B. R.; Colton, R.; McCormick, M. J. *J. Chem. Soc., Chem. Commun.* **1976**, 485.
(8) Kubiak, C. P.; Eisenberg, R. *J. Am. Chem. Soc.* **1980**, *102*, 3637.
(9) Mague, J. T.; DeVries, S. H. *Inorg. Chem.* **1980**, *19*, 3743.
(10) Kubiak, C. P.; Woodcock, C.; Eisenberg, R. *Inorg. Chem.* **1980**, *19*, 2733.
(11) Farr, J. P.; Olmstead, M. M.; Balch, A. L. *J. Am. Chem. Soc.* **1980**, *102*, 6654.
(12) Balch, A. L.; Benner, L. S.; Olmstead, M. M. *Inorg. Chem.* **1979**, *18*, 2996.
(13) Brown, M. P.; Puddephatt, R. J.; Rashidi, M.; Seddon, K. R. *Inorg. Chim. Acta* **1977**, *23*, L27, L33.
(14) Cowie, M.; Mague, J. T.; Sanger, A. R. *J. Am. Chem. Soc.* **1978**, *100*, 3628.
(15) Anderson, M. P.; Mattson, B. M.; Pignolet, L. H. *Inorg. Chem.*, in press.
(16) Dahlhoff, W. V.; Dick, T. R.; Ford, G. H.; Kelly, W. S. J.; Nelson, S. M. *J. Chem. Soc. A* **1971**, 3495.

0020-1669/83/1322-3267$01.50/0 © 1983 American Chemical Society

121.5 MHz and at 25 °C by use of a Nicolet NT-300 spectrometer. The chemical shifts are reported in ppm relative to the external standard 85% H_3PO_4 with positive shifts downfield. ^1H NMR spectra were recorded by use of the same instrument. IR spectra were recorded with a Beckman Model 4250 grating spectrometer by use of KBr disks unless noted otherwise, and UV–vis spectra were recorded by use of CH_2Cl_2 solutions with a Cary Model 17 spectrometer.

Preparation of Compounds. All manipulations were carried out under a purified N_2 atmosphere using standard Schlenk techniques. $[(C_6H_5)_2P]_2CHC_5H_4N$ (PNP) and $[Rh(nbd)(PNP)]PF_6$ (nbd = norbornadiene) were prepared according to literature methods.[15]

$[Rh_2(CO)_2(PNP)_2](PF_6)_2 \cdot C_3H_6O$ (1) was prepared by the reaction of $[Rh(nbd)(PNP)]PF_6$ with carbon monoxide (1 atm) in acetone solution. The initial yellow solution immediately changed to purple. The solution was stirred at room temperature for 20 min. Dark purple, octahedral-shaped crystals were obtained by solvent diffusion with acetone and pentane: yield 90%. $^{31}P\{^1H\}$ NMR (acetone): $\delta_1 = 62.0$ (d of d of d, int = 1), $J_{P-P(trans)} = 293.5$ Hz, $J_{Rh-P} = 117.9$ Hz, $J_{P-P} = 54.1$ Hz; $\delta_2 = 40.2$ (d of d of d, int = 1), $J_{P-P(trans)} = 293.0$ Hz, $J_{Rh-P} = 134.3$ Hz, $J_{P-P} = 54.0$ Hz. IR (cm^{-1}, CH_2Cl_2): $\nu(CO) = 2002$ (br), ν(py CN) = 1602. UV–vis (λ, nm (log ϵ)): 370 sh (3.114), 522 (3.633). Anal. Calcd for $C_{62}H_{50}F_{12}N_2O_2P_6Rh_2$: C, 50.92; H, 3.68; N, 1.83; P, 12.12. Found: C, 50.63; H, 3.55; N, 1.83; P, 12.44.

$[Ir(cod)(PNP)]BF_4$ (cod = cyclooctadiene) was obtained as a yellow powder by reaction of PNP ligand (0.96 mmol) dissolved in 25 mL of toluene with the filtrate of the reaction of $[Ir(cod)Cl]_2$ (0.48 mmol) with $AgBF_4$ (1.00 mmol) in acetone. The solid that formed upon vacuum distillation of the solvent was filtered and washed with methanol. Yellow crystals were obtained by solvent diffusion by use of dichloromethane and diethyl ether: yield 85%. $^{31}P\{^1H\}$ NMR (CH_2Cl_2): δ 9.6 (s). IR (cm^{-1}): ν(py CN) = 1595. Anal. Calcd for $C_{38}H_{37}BF_4NP_2$: C, 53.73; H, 4.36; N, 1.65; P, 7.31. Found: C, 53.59; H, 4.51; N, 1.60; P, 6.99.

$[Ir_2(\mu\text{-}CO)(CO)_2(PNP)_2](BF_4)_2$ (2) was prepared by reaction of an acetone solution of $[Ir(cod)(PNP)]BF_4$ with CO (1 atm) at room temperature. The pale yellow solution darkened to orange-yellow, and when this solution was layered with pentane, yellow crystals separated. The solution must be kept under an atmosphere of CO in order to prevent loss of the bridging CO in **2** (vide infra). The product of this reaction is often contaminated with green crystals of $[Ir(CO)(PNP)]_2(BF_4)_2$. Physical separation with the aid of a microscope is usually necessary to assure product purity. $^{31}P\{^1H\}$ NMR (acetone) shows a complex symmetric pattern centered at δ 28.1 that is best described as an appropriate quartet of triplets (Figure S1, included as supplementary material). IR (cm^{-1}, CH_2Cl_2 solution): $\nu(CO) = 2075$ (w), 2025 (w), 1984 (s), 1788 (m); ν(py CN) = 1596 (m), 1586 (m). IR (cm^{-1}, KBr disk): $\nu(CO) = 1994$ (sh), 1984 (s), 1964 (s), 1803 (s); ν(py CN) = 1595. The UV–vis spectrum (CH_2Cl_2 solution) was featureless in the visible and near-IR regions (350–1500 nm) and consisted of a gradual tailing from intense absorptions in the UV below 310 nm. Anal. Calcd for $C_{63}H_{50}B_2F_8N_2O_3P_4Ir_2$: C, 48.30; H, 3.19; N, 1.79; P, 7.92. Found: C, 48.02; H, 3.33; N, 1.69; P, 7.80. **$[Ir(CO)(PNP)]_2(BF_4)_2$ (3)** is best prepared by purging an orange-yellow acetone solution of **2** with N_2 in order to remove excess CO. The solution slowly became dark green. Green crystals were obtained by layering with pentane, and any yellow crystals of **2** were removed under a microscope. $^{31}P\{^1H\}$ NMR (CH_2Cl_2) shows an unsymmetric broadened pattern centered at ca. δ 30 (Figure S2, included as supplementary material). IR (cm^{-1}, CH_2Cl_2 solution): $\nu(CO) = 2019$ (m), 1958 (s); ν(py CN) = 1584. IR (cm^{-1}, KBr disk): $\nu(CO) = 2005$ (s), 1981 (sh), 1964 (s); ν(py CN) = 1600. UV–vis (λ, nm (log ϵ)): 344 (3.75), 410 (3.53), 444 sh (3.39), 617 (3.85). Anal. Calcd for $C_{62}H_{50}B_2F_8N_2O_2P_4Ir_2$: C, 48.40; H, 3.25; N, 1.82; P, 8.07. Found: C, 48.16; H, 3.52; N, 1.84; P, 7.83.

$Rh_2(\mu\text{-}S)(CO)_2(PNP)_2$ (4). Dry sodium sulfide (0.066 mmol) dissolved in 5 mL of dry methanol was added to a purple slurry of **1** (0.060 mmol) in methanol. A red precipitate formed immediately, and the reaction mixture was stirred for 1 h. The precipitate was collected by filtration and washed with dry methanol. Small red crystals of the product were obtained by solvent diffusion with acetone and hexane: yield 75%. $^{31}P\{^1H\}$ NMR ($CDCl_3$): δ 34.1 (symmetric multiplet with two principal lines separated by ca. 139 Hz). IR (cm^{-1}): $\nu(CO) = 1930$, 1948; ν(py CN) = 1582. UV–vis (λ, nm (log ϵ)): 310 (4.114), 375 (3.568), 464 (3.612). Anal. Calcd for $C_{62}H_{50}N_2O_2P_4SRh_2$: C, 61.20; H, 4.14; N, 2.30. Found: C, 58.68; H, 4.35; N, 2.06.

Rh(CO)(Cl)(PNP) (5). Complex **1** (30.4 mg, 0.0224 mmol) was dissolved in 5 mL of dry acetone. A saturated acetone solution of $NEt_4Cl \cdot H_2O$ was added dropwise until the purple color due to the starting rhodium compound had turned canary yellow. The solution was dried over anhydrous sodium sulfate for 1 h and filtered into a round-bottom flask. The solution was cooled to −78 °C and layered with 25 mL of hexane. Solvent diffusion was allowed to proceed at room temperature for 24 h, which afforded a powdery yellow material along with numerous large yellow crystals. Solvents were syringed off and the solids dried by a gentle stream of N_2. The large crystals were manually separated from the solid products and yielded 10.6 mg (38%) of **5**. $^{31}P\{^1H\}$ NMR (acetone): $\delta_1 = 69.1$ (d of d, int = 1), $J_{Rh-P} = 168$ Hz, $J_{P-P'} = 107$ Hz; $\delta_2 = 0.35$ (d, int = 1), $J_{P-P'} = 108$ Hz. IR (cm^{-1}): $\nu(CO) = 1990$; ν(py CN) = 1601. UV–vis (acetone) (λ, nm (log ϵ)): 370 sh (3.041), 355 sh, (3.643). Anal. Calcd for $C_{31}H_{25}ClNORh$: C, 59.30; H, 4.01; N, 2.23. Found: C, 59.91; H, 4.24; N, 2.24.

$[Ir_2(CO)_2(I)(PNP)_2](BF_4)$ (6). One equivalent of NBu_4I dissolved in acetone was added to a green acetone solution of **3**. The solution immediately turned yellow. The solvent was removed in vacuo, and the remaining yellow solid was washed with H_2O. Crystals were obtained by recrystallization from a CH_2Cl_2/hexane solvent mixture: yield 78%. Anal. Calcd for $C_{62}H_{50}BF_4N_2O_2P_4IIr_2 \cdot CH_2Cl_2$: C, 45.4; H, 3.13; N, 1.68; P, 7.46; I, 7.64. Found: C, 45.5; H, 3.47; N, 1.63; P, 7.46; I, 7.64. IR (cm^{-1}): $\nu(CO) = 2008$, 1956 (KBr disk) and 2020, 1960 (CH_2Cl_2 solution); ν(py CN) = 1604, 1584 (KBr disk) and 1606, 1586 (CH_2Cl_2 solution). $^{31}P\{^1H\}$ NMR (CH_2Cl_2 solvent) shows four well-separated multiplets, each a doublet of doublets of doublets, centered at δ 8.83, 18.5, 31.6, and 39.2. A trace of this spectrum is included as supplementary material.

Collection and Reduction of X-ray Data. A summary of crystal and intensity data for compounds **1** and **2** is presented in Table I. Crystals of both compounds were secured to the end of glass fibers with 5-min epoxy resin. The crystal class of each compound was determined by use of the Enraf-Nonius CAD 4-SDP peak search, centering, and indexing programs.[17] Background counts were measured at both ends of the scan range with the use of an ω–2θ scan, equal, at each side, to one-fourth of the scan range of the peak. In this manner, the total duration of background measurements is equal to half of the time required for the peak scan. The intensities of three standard reflections were measured every 1.5 h of X-ray exposure, and no decay with time was noted for either compound. The data were corrected for Lorentz, polarization, and background effects. An empirical absorption correction was applied for compound **2** by use of ψ-scan data and the programs PSI and EAC.[17]

Solution and Refinement of the Structures. Both structures were solved by conventional heavy-atom techniques. The metal atoms were located by Patterson syntheses. Full-matrix least-squares refinement and difference-Fourier calculations were used to locate all remaining non-hydrogen atoms. The atomic scattering factors were taken from the usual tabulation,[18] and the effects of anomalous dispersion were included in F_c by using Cromer and Ibers'[19] values of $\Delta f'$ and $\Delta f''$. Tables of observed and calculated structure factor amplitudes are available.[20] Hydrogen atom positions were calculated (C–H distance set at 0.95 Å) for the dication of **1** and were included in structure factor calculations but were not refined. The PF_6 anion for **1** was found to possess a disorder such that four of the six fluorine atoms each showed two rotationally related positions. A satisfactory model was found by refining the multiplicities of these eight positions. The results are summarized in Table II. The acetone solvate molecule of compound **1** was found to be disordered about an inversion center that is located approximately at the midpoint of the CO bond. Since this is an unimportant part of the structure, a simple model in which the three positions were called carbon atoms with appropriate mul-

---

(17) All calculations were carried out on PDP 8A and 11/34 computers with use of the Enraf-Nonius CAD 4-SDP programs. This crystallographic computing package is described by: Frenz, B. A. In "Computing in Crystallography"; Schenk, H., Olthof-Hazekamp, R., van Koningsveld, H., Bassi, G. C., Eds.; Delft University Press: Delft, Holland, 1978; pp 64–71. "CAD 4 and SDP User's Manual"; Enraf-Nonius: Delft, Holland, 1978.

(18) Cromer, D. T.; Waber, J. T. "International Tables for X-ray Crystallography"; Kynoch Press: Birmingham, England, 1974; Vol. IV, Table 2.2.4. Cromer, D. T. *Ibid.*, Table 2.3.1.

(19) Cromer, D. T.; Ibers, J. A. In ref 18.

(20) See paragraph at end of paper regarding supplementary material.

Table I. Summary of Crystal Data and Intensity Collection for Compounds 1 and 2

	1	2
	Crystal Parameters	
cryst syst	orthorhombic	triclinic
space group	*Pbcn* (No. 60)	$P\bar{1}$ (No. 2)
cell parameters		
a, Å	19.658 (7)	16.387 (4)
b, Å	18.528 (7)	16.710 (6)
c, Å	17.993 (6)	24.710 (6)
α, deg	90	76.03 (2)
β, deg	90	84.16 (2)
γ, deg	90	75.37 (2)
V, $Å^3$	6554 (7)	6347 (4)
Z	4	4
calcd density, g cm^{-3}	1.553	1.638
abs coeff, cm^{-1}	7.2	46.0
max, min, av transmission factors		1.0, 0.69, 0.88
formula	$C_{62}H_{50}F_{12}N_2O_2P_6Rh_2 \cdot C_3H_6O$	$C_{63}H_{50}B_2F_8N_2O_3P_4Ir_2$
fw	1532.8	1565.0
	Measurement of Intensity Data	
diffractometer	CAD 4	CAD4
radiation	Mo $K\bar{\alpha}$ (λ = 0.710 69 Å) graphite monochromatized	Mo$K\bar{\alpha}$ graphite monochromatized
scan range, 2θ, deg	0–50	0–44
unique reflcns measd (region)	5140 (+*h*, +*k*, +*l*)	15 397 (+*h*, ±*k*, ±*l*)
obsd reflcns[a]	3317 [$F_o^2 \geqslant \sigma(F_o^2)$]	8284 [$F_o^2 \geqslant 3\sigma(F_o^2)$]
refinement by full matrix least-squares		
no. of parameters	388	818
R^b	0.040	0.043
$R_w{}^b$	0.043	0.058
GOF[b]	1.34	1.68
p^a	0.04	0.04

[a] The intensity data were processed as described in: "CAD4 and SDP User's Manual"; Enraf-Nonius: Delft, Holland, 1978. The net intensity $I = [K/(\text{NPI})](C - 2B)$, where $K = 20.1166 \times$ (attenuator factor) NPI = ratio of fastest possible scan rate to scan rate for the measurement, C = total count, and B = total background count. The standard deviation in the net intensity is given by $[\sigma(I)]^2 = (K/(\text{NPI}))^2[C + 4B + (pI)^2]$, where p is a factor used to downweight intense reflections. The observed structure factor amplitude F_o is given by $F_o = (I/Lp)^{1/2}$, where Lp = Lorentz and polarization factors. The $\sigma(I)$'s were converted to the estimated errors in the relative structure factors $\sigma(F_o)$ by $\sigma(F_o) = {}^1/_2[\sigma(I)/I]F_o$. [b] The function minimized was $\Sigma w(|F_o| - |F_c|)^2$, where $w = 1/[\sigma(F_o)]^2$. The unweighted and weighted residuals are defined as $R = (\Sigma||F_o| - |F_c||)/\Sigma|F_o|$ and $R_w = [(\Sigma w(|F_o| - |F_c|))^2/(\Sigma w|F_o|)^2]^{1/2}$. The error in an observation of unit weight (GOF) is $[\Sigma w(|F_o| - |F_c|)^2/(\text{NO} - \text{NV})]^{1/2}$, where NO and NV are the number of observations and variables, respectively.

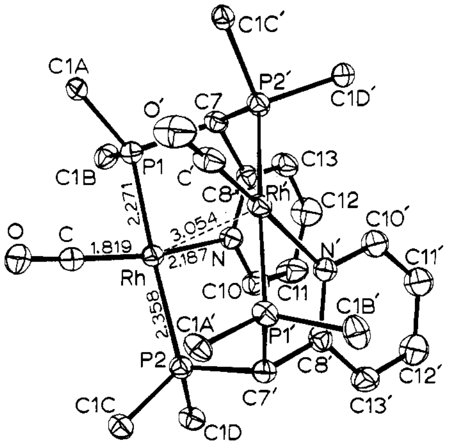

Figure 1. ORTEP drawing of the dication $[Rh_2(CO)_2(PNP)_2]^{2+}$ (**1**), showing the labeling scheme. Phenyl ring carbon atoms have been omitted for clarity and are labeled C1 through C6 for each ring A through D, and primed atoms are related to their unprimed counterparts by C_2 symmetry ($x, y, z, \rightarrow -x, y, {}^1/_2 - z$). The thermal ellipsoids show 35% probability surfaces.

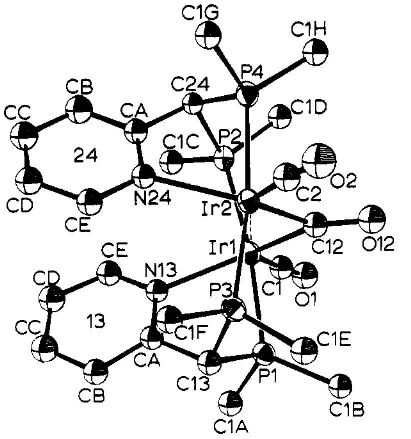

Figure 2. ORTEP drawing of the A dication of $[Ir_2(\mu\text{-}CO)(CO)_2(PNP)_2]^{2+}$ (**2**), showing the labeling scheme. Phenyl ring carbon atoms have been omitted for clarity and are labeled C1 through C6 for each ring A through H. Dication B is labeled in an identical manner. The thermal ellipsoids show 35% probability surfaces.

tiplicities was used to account for this disorder (see Table II).

The crystal structure of **2** possesses two entire dications in the asymmetric unit. Although the structures of these two dications are very similar, a careful examination of the packing shows that they are unambiguously not related by crystallographic symmetry of some higher order unit cell.

The final difference-Fourier maps for both compounds did not reveal chemically significant residual electron density. The final positional and thermal parameters of the refined atoms appear in Tables II and III and as supplementary material.[20] The labeling schemes for both compounds are presented in Figures 1 and 2.

Results and Discussion

Synthesis and Spectroscopic Characterization of the Binuclear Complexes. The reaction of $[Rh(nbd)(PNP)]PF_6$[15] with CO at 1 atm and 25 °C in acetone solution leads to nearly quantitative formation of the binuclear complex $[Rh_2(CO)_2(PNP)_2](PF_6)_2$ (**1**), which crystallized as an acetone monosolvate. Complex **1** has a deep purple color, and its formulation is based on IR and ^{31}P NMR spectroscopy and on a single-

Table II. Positional and Thermal Parameters and Their Esd's for $[Rh_2(CO)_2(PNP)_2](PF_6)_2 \cdot C_3H_6O$ (1)

atom	x	y	z	B_{iso}, A^2 [a]
Rh	0.06049 (2)	0.21793 (2)	0.19674 (2)	2.839
P1	−0.00547 (7)	0.20344 (7)	0.09421 (8)	3.047
P2	0.12757 (6)	0.24014 (6)	0.30294 (8)	2.888
P3	0.30594 (10)	0.11095 (11)	0.07872 (11)	6.555
F1	0.2861 (3)	0.0466 (3)	0.1287 (3)	13.048
F2	0.3293 (2)	0.1768 (2)	0.0278 (2)	9.106
F3[b]	0.2445 (3)	0.1557 (4)	0.1093 (3)	9.454
F4[b]	0.3672 (4)	0.0655 (4)	0.0464 (4)	12.452
F5[b]	0.3488 (4)	0.1349 (5)	0.1455 (4)	11.382
F6[b]	0.2587 (4)	0.0849 (4)	0.0099 (3)	10.254
F7[b]	0.3856 (8)	0.1050 (9)	0.0996 (10)	11.0 (5)
F8[b]	0.3123 (9)	0.1701 (10)	0.1438 (10)	11.8 (5)
F9[b]	0.3162 (8)	0.0648 (8)	0.0183 (9)	10.5 (4)
F10[b]	0.2363 (11)	0.1356 (10)	0.0690 (11)	14.0 (6)
O	0.1039 (2)	0.0654 (2)	0.1907 (2)	5.671
N	0.0253 (2)	0.3277 (2)	0.1741 (2)	3.108
C	0.0882 (3)	0.1243 (3)	0.1943 (3)	3.731
C7	−0.0740 (2)	0.2697 (2)	0.1168 (3)	3.015
C8	−0.0329 (2)	0.3371 (3)	0.1351 (3)	3.245
C10	0.0633 (3)	0.3870 (3)	0.1866 (3)	4.146
C11	0.0463 (3)	0.4542 (3)	0.1614 (4)	5.206
C12	−0.0127 (3)	0.4630 (3)	0.1217 (4)	5.577
C13	−0.0529 (3)	0.4038 (3)	0.1085 (3)	4.228
C1A	−0.0418 (2)	0.1184 (3)	0.0647 (3)	3.112
C2A	−0.0604 (3)	0.1077 (3)	−0.0096 (3)	4.471
C3A	−0.0905 (3)	0.0437 (3)	−0.0306 (4)	5.868
C4A	−0.1021 (3)	−0.0091 (3)	0.0213 (4)	6.156
C5A	−0.0825 (3)	0.0004 (3)	0.0938 (4)	5.418
C6A	−0.0524 (3)	0.0642 (3)	0.1167 (3)	3.981
C1B	0.0341 (3)	0.2396 (3)	0.0117 (3)	3.827
C2B	0.1026 (3)	0.2205 (3)	−0.0002 (4)	5.515
C3B	0.1363 (4)	0.2419 (4)	−0.0621 (4)	8.515
C4B	0.1027 (4)	0.2847 (4)	−0.1129 (4)	10.094
C5B	0.0368 (4)	0.3067 (4)	−0.1023 (4)	8.153
C6B	0.0011 (3)	0.2828 (3)	−0.0396 (3)	5.667
C1C	0.1851 (2)	0.1716 (3)	0.3423 (3)	3.016
C2C	0.2236 (2)	0.1320 (3)	0.2923 (3)	3.796
C3C	0.2714 (3)	0.0828 (3)	0.3179 (3)	4.826
C4C	0.2812 (3)	0.0737 (3)	0.3927 (4)	5.316
C5C	0.2439 (3)	0.1139 (3)	0.4424 (3)	5.053
C6C	0.1966 (3)	0.1647 (3)	0.4178 (3)	3.950
C1D	0.1905 (2)	0.3110 (3)	0.2875 (3)	3.356
C2D	0.2171 (3)	0.3534 (3)	0.3428 (3)	3.964
C3D	0.2675 (3)	0.4030 (3)	0.3264 (4)	5.542
C4D	0.2910 (3)	0.4100 (3)	0.2549 (4)	6.797
C5D	0.2671 (3)	0.3664 (4)	0.1995 (4)	6.788
C6D	0.2164 (3)	0.3171 (3)	0.2154 (3)	4.760
CS1[c]	0.4761 (9)	0.352 (1)	0.222 (1)	8.6 (5)
CS2[c]	0.4376 (13)	0.308 (1)	0.218 (1)	12.2 (7)
CS3[c]	0.4725 (14)	0.405 (1)	0.214 (1)	14.2 (9)

[a] Anisotropic thermal parameters are included as supplementary material. [b] Disordered F atoms: F2–F6 have multiplicities of 0.65 and F7–F10 have multiplicities of 0.35. [c] Disordered acetone solvate atoms, multiplicity 0.50 (see text).

crystal X-ray analysis (vide infra). The IR spectrum (CH_2Cl_2 solution) of 1 contains one metal carbonyl stretch, ν(CO) = 2002 cm^{-1}, and a pyridyl C–N stretch, ν(py CN) = 1602 cm^{-1}. The ν(py CN) stretching frequency generally provides direct evidence regarding coordination of the pyridyl nitrogen atom. In free PNP the stretch comes at 1580 cm^{-1} and upon coordination the frequency is increased to ca. 1600 cm^{-1} or higher.[15,16] The value of 1602 cm^{-1} observed in 1 suggests that the pyridyl nitrogen atom is coordinated. The $^{31}P\{^1H\}$ NMR spectrum (acetone) consists of two well-separated multiplets of equal intensity (δ_1 = 62.0 and δ_2 = 40.2), each a doublet of doublet of doublets (see Experimental Section). These data suggest that the solution structure of 1 is that of a binuclear dimer of the face-to-face variety with the two PNP ligands bridging via their phosphorus atoms and with the nitrogen atoms coordinated trans to the carbonyls. The structure shown for 1 is consistent with these data and has been confirmed in the solid state by an X-ray analysis (vide infra). Complex 1 is the first face-to-face dimer of this type with the cis-carbonyl arrangement.

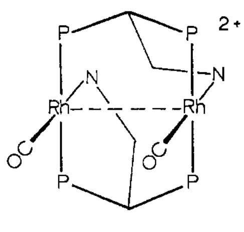

1

The reaction of PNP ligand with $[Ir(cod)(Cl)]_2$ and $AgBF_4$ in an acetone/toluene solution leads to the formation of $[Ir(cod)(PNP)]BF_4$ in good yield. This yellow complex is analogous to $[Rh(nbd)(PNP)]BF_4$, in which the PNP ligand is tridentate.[15] In this Rh complex ν(py CN) = 1600 cm^{-1} and the Rh–N separation is 2.148 (5) Å.[15] In $[Ir(cod)(PNP)]BF_4$, ν(py CN) = 1595 cm^{-1} compared with 1580 cm^{-1} for the free PNP ligand, and a singlet is observed in the $^{31}P\{^1H\}$ NMR spectrum (δ 9.6). These data suggest that the iridium and rhodium complexes have similar structures.

The reaction of $[Ir(cod)(PNP)]BF_4$ with CO at 1 atm and 25 °C in acetone solution leads to a darkening of the yellow color to orange. Two complexes may be isolated from this solution. $[Ir_2(\mu\text{-}CO)(CO)_2(PNP)_2](BF_4)_2$ (2) is obtained in good yield as yellow crystals if the solution is maintained under an atmosphere of CO during crystallization. If the excess CO is removed via a purge of N_2, the green complex $[Ir_2(CO)_2(PNP)_2](BF_4)_2$ (3) is obtained upon crystallization. These two complexes may be readily interconverted numerous times by bubbling CO and N_2, sequentially, through an acetone solution of 2 or 3. The structure of complex 3 is probably similar to that of 1 as judged by IR and ^{31}P NMR spectroscopy; however, isomers with the pyridyl nitrogen atom unbound are probably present. In complex 3, ν(py CN) = 1600 cm^{-1} and ν(CO) = 2005, 1964 cm^{-1} in the solid, but note that in CH_2Cl_2 solution a ν(py CN) band at 1584 cm^{-1} is present. The $^{31}P\{^1H\}$ NMR shows a complex broadened pattern centered at δ 34 (spectrum included as supplementary material[20]). The broadening in this spectrum could be due to a fluxional process involving Ir–N bond breaking. These data are consistent with a solid-state structure similar to that of 1 but with a solution structure that probably includes an unbound N atom. Further support for this structure is provided by the X-ray diffraction analysis of complex 2 (vide infra). The structures of 2 and 3 must be related since 2 is readily formed by the addition of CO to 3. The structure of 2 is that of a binuclear PNP-bridged dimer with one bridging CO and two terminal CO ligands. It is easy to envision the addition of a CO molecule to the iridium

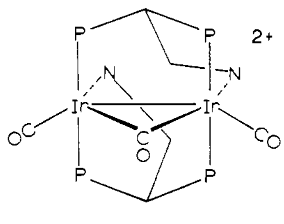

2

Table III. Positional and Thermal Parameters and Their Esd's for $[Ir_2(\mu\text{-}CO)(CO)_2(PNP)_2]^{2+}$ (2)[a]

dication A					dication B				
atom	x	y	z	B_{iso}, Å^2	atom	x	y	z	B_{iso}, Å^2
Ir1[b]	0.00463 (4)	0.08726 (4)	0.11991 (3)	2.850	Ir1	0.45197 (4)	0.46393 (4)	0.36550 (3)	2.806
Ir2[b]	0.10210 (4)	0.01944 (4)	0.21489 (3)	2.851	Ir2	0.34196 (4)	0.56886 (4)	0.28265 (3)	2.817
P1[b]	−0.1140 (3)	0.0388 (3)	0.1584 (2)	3.175	P1	0.5711 (3)	0.5124 (3)	0.3293 (2)	3.033
P2[b]	0.1123 (3)	0.1561 (2)	0.0795 (2)	3.234	P2	0.3426 (3)	0.3967 (3)	0.4017 (2)	3.097
P3[b]	−0.0227 (3)	−0.0001 (3)	0.2666 (2)	3.150	P3	0.4624 (3)	0.5973 (3)	0.2281 (2)	3.282
P4[b]	0.2274 (3)	0.0516 (3)	0.1738 (2)	3.239	P4	0.2187 (3)	0.5345 (3)	0.3257 (2)	3.034
O1	−0.0405 (7)	0.0878 (7)	0.0047 (5)	5.4 (3)	O1	0.5239 (8)	0.4157 (7)	0.4784 (5)	5.8 (3)
O2	0.1980 (8)	−0.1269 (7)	0.2958 (5)	5.8 (3)	O2	0.2417 (8)	0.7380 (8)	0.2241 (5)	6.1 (3)
O12	0.1074 (7)	−0.0920 (7)	0.1354 (5)	4.7 (3)	O12	0.3650 (7)	0.6390 (6)	0.3785 (4)	4.2 (2)
N13	−0.0725 (8)	0.1843 (7)	0.1687 (5)	3.4 (3)	N13	0.5124 (8)	0.3894 (7)	0.2961 (5)	3.6 (3)
N24	0.0912 (8)	0.1602 (7)	0.2165 (5)	3.4 (3)	N24	0.3360 (7)	0.4424 (7)	0.2619 (5)	3.1 (3)
C1	−0.0248 (10)	0.0919 (10)	0.0506 (7)	4.1 (4)	C1	0.4976 (10)	0.4307 (9)	0.4342 (6)	3.5 (3)
C2	0.1600 (10)	−0.0668 (10)	0.2659 (7)	4.0 (4)	C2	0.2799 (11)	0.6720 (10)	0.2459 (7)	4.6 (4)
C12	0.0813 (10)	−0.0259 (9)	0.1513 (7)	3.9 (4)	C12	0.3796 (9)	0.5834 (8)	0.3546 (6)	2.9 (3)
C13	−0.1197 (10)	0.0616 (9)	0.2291 (6)	3.7 (3)	C13	0.5612 (10)	0.5199 (9)	0.2526 (6)	3.4 (3)
C24	0.1854 (9)	0.1596 (8)	0.1324 (6)	2.9 (3)	C24	0.2585 (9)	0.4177 (9)	0.3512 (6)	3.0 (3)
C13A	−0.1204 (10)	0.1553 (9)	0.2129 (6)	3.5 (3)	C13A	0.5564 (10)	0.4303 (9)	0.2539 (6)	3.6 (3)
C13B	−0.1783 (10)	0.2093 (9)	0.2431 (7)	3.9 (4)	C13B	0.6012 (11)	0.3882 (10)	0.2137 (7)	4.4 (4)
C13C	−0.1790 (11)	0.2980 (10)	0.2263 (7)	4.7 (4)	C13C	0.5975 (12)	0.3022 (11)	0.2181 (8)	5.6 (5)
C13D	−0.1274 (11)	0.3279 (10)	0.1816 (7)	4.8 (4)	C13D	0.5529 (12)	0.2637 (11)	0.2607 (8)	5.2 (4)
C13E	−0.0766 (10)	0.2682 (10)	0.1529 (7)	4.1 (4)	C13E	0.5084 (10)	0.3076 (10)	0.3008 (7)	4.3 (4)
C24A	0.1355 (10)	0.2046 (9)	0.1761 (6)	3.6 (3)	C24A	0.2946 (10)	0.3914 (9)	0.2986 (6)	3.5 (3)
C24B	0.1396 (11)	0.2889 (10)	0.1729 (7)	4.8 (4)	C24B	0.2828 (10)	0.3173 (10)	0.2872 (7)	4.1 (4)
C24C	0.0940 (11)	0.3268 (10)	0.2171 (7)	4.7 (4)	C24C	0.3165 (11)	0.2970 (10)	0.2371 (7)	4.6 (4)
C24D	0.0506 (11)	0.2820 (10)	0.2570 (7)	4.3 (4)	C24D	0.3600 (10)	0.3470 (10)	0.1991 (7)	4.3 (4)
C24E	0.0487 (10)	0.1991 (9)	0.2570 (7)	3.9 (4)	C24E	0.3699 (10)	0.4226 (9)	0.2119 (6)	3.8 (4)
C1A	−0.2144 (11)	0.1092 (10)	0.1294 (7)	4.2 (4)	C1A	0.6694 (10)	0.4311 (9)	0.3460 (6)	3.6 (3)
C2A	−0.2910 (12)	0.0865 (11)	0.1510 (8)	5.3 (4)	C2A	0.7456 (11)	0.4548 (10)	0.3296 (7)	4.7 (4)
C3A	−0.3673 (12)	0.1384 (12)	0.1293 (8)	6.1 (5)	C3A	0.8236 (11)	0.3924 (11)	0.3425 (8)	5.2 (4)
C4A	−0.3659 (14)	0.2074 (13)	0.0883 (9)	7.1 (6)	C4A	0.8210 (11)	0.3079 (11)	0.3697 (8)	5.2 (4)
C5A	−0.2914 (13)	0.2304 (12)	0.0670 (9)	6.6 (5)	C5A	0.7448 (13)	0.2850 (12)	0.3841 (9)	6.6 (5)
C6A	−0.2134 (11)	0.1793 (11)	0.0886 (7)	5.1 (4)	C6A	0.6693 (12)	0.3504 (11)	0.3705 (8)	5.2 (4)
C1B	−0.1213 (10)	−0.0699 (9)	0.1608 (6)	3.5 (3)	C1B	0.5907 (9)	0.6083 (9)	0.3426 (6)	3.4 (3)
C2B	−0.0755 (10)	−0.1034 (9)	0.1170 (6)	3.4 (3)	C2B	0.5582 (11)	0.6287 (10)	0.3927 (7)	4.7 (4)
C3B	−0.0864 (11)	−0.1865 (11)	0.1156 (7)	5.1 (4)	C3B	0.5749 (12)	0.6981 (11)	0.4086 (8)	5.4 (4)
C4B	−0.1403 (12)	−0.2251 (11)	0.1516 (8)	5.5 (5)	C4B	0.6250 (12)	0.7441 (12)	0.3733 (8)	6.0 (5)
C5B	−0.1846 (12)	−0.1898 (11)	0.1934 (8)	5.8 (5)	C5B	0.6606 (12)	0.7243 (11)	0.3220 (8)	5.8 (5)
C6B	−0.1771 (11)	−0.1095 (11)	0.1990 (7)	5.1 (4)	C6B	0.6422 (11)	0.6567 (10)	0.3052 (7)	4.7 (4)
C1C	0.0733 (11)	0.2656 (10)	0.0421 (7)	4.3 (4)	C1C	0.3728 (10)	0.2815 (9)	0.4209 (6)	3.7 (3)
C2C	0.1244 (12)	0.3232 (11)	0.0332 (8)	5.6 (5)	C2C	0.3159 (11)	0.2319 (10)	0.4245 (7)	4.4 (4)
C3C	0.1001 (14)	0.4034 (13)	−0.0074 (9)	7.5 (6)	C3C	0.3378 (13)	0.1443 (13)	0.4452 (9)	6.8 (5)
C4C	0.0262 (13)	0.4204 (12)	−0.0347 (9)	6.7 (5)	C4C	0.4213 (16)	0.1035 (15)	0.4589 (11)	9.1 (7)
C5C	−0.0300 (13)	0.3682 (12)	−0.0236 (8)	6.4 (5)	C5C	0.4818 (16)	0.1524 (15)	0.4559 (11)	9.0 (7)
C6C	−0.0034 (11)	0.2869 (11)	0.0159 (7)	5.0 (4)	C6C	0.4559 (11)	0.2444 (11)	0.4367 (8)	5.2 (4)
C1D	0.1830 (10)	0.1119 (10)	0.0267 (7)	4.1 (4)	C1D	0.2868 (10)	0.4245 (9)	0.4651 (6)	3.7 (3)
C2D	0.1825 (11)	0.0301 (10)	0.0200 (7)	4.5 (4)	C2D	0.2975 (10)	0.4944 (10)	0.4829 (7)	4.1 (4)
C3D	0.2413 (12)	−0.0038 (11)	−0.0209 (8)	5.2 (4)	C3D	0.2530 (11)	0.5140 (10)	0.5318 (7)	4.6 (4)
C4D	0.2940 (13)	0.0424 (12)	−0.0519 (9)	6.5 (5)	C4D	0.1995 (12)	0.4683 (11)	0.5603 (8)	5.6 (5)
C5D	0.2936 (13)	0.1249 (12)	−0.0472 (8)	6.5 (5)	C5D	0.1876 (12)	0.3993 (12)	0.5438 (8)	6.1 (5)
C6D	0.2368 (12)	0.1599 (11)	−0.0059 (8)	5.3 (4)	C6D	0.2305 (11)	0.3757 (10)	0.4950 (7)	4.5 (4)
C1E	−0.0366 (10)	−0.1054 (9)	0.2866 (7)	3.9 (4)	C1E	0.4843 (10)	0.7005 (9)	0.2242 (6)	3.8 (4)
C2E	−0.0982 (11)	−0.1280 (11)	0.3276 (7)	5.0 (4)	C2E	0.5488 (12)	0.7252 (11)	0.1862 (8)	5.2 (4)
C3E	−0.1142 (13)	−0.2119 (12)	0.3419 (9)	6.6 (5)	C3E	0.5661 (12)	0.8050 (12)	0.1841 (8)	5.8 (5)
C4E	−0.0638 (12)	−0.2741 (11)	0.3155 (8)	5.8 (5)	C4E	0.5195 (13)	0.8573 (12)	0.2186 (8)	6.4 (5)
C5E	0.0002 (11)	−0.2541 (10)	0.2757 (7)	4.7 (4)	C5E	0.4575 (12)	0.8328 (11)	0.2531 (8)	5.6 (5)
C6E	0.0154 (10)	−0.1715 (10)	0.2609 (7)	4.3 (4)	C6E	0.4358 (10)	0.7520 (10)	0.2588 (7)	4.0 (4)
C1F	−0.0355 (10)	0.0313 (9)	0.3320 (7)	3.8 (4)	C1F	0.4584 (11)	0.5933 (10)	0.1564 (7)	4.3 (4)
C2F	−0.1171 (11)	0.0570 (11)	0.3584 (7)	4.9 (4)	C2F	0.5344 (12)	0.5763 (12)	0.1238 (8)	5.9 (5)
C3F	−0.1231 (12)	0.0749 (11)	0.4129 (8)	5.8 (5)	C3F	0.5292 (14)	0.5786 (13)	0.0645 (9)	7.5 (6)
C4F	−0.0494 (12)	0.0743 (12)	0.4372 (8)	6.2 (5)	C4F	0.4503 (14)	0.5922 (13)	0.0420 (9)	7.1 (6)
C5F	0.0315 (13)	0.0472 (12)	0.4130 (8)	6.4 (5)	C5F	0.3780 (13)	0.6128 (13)	0.0743 (9)	6.7 (5)
C6F	0.0385 (11)	0.0276 (10)	0.3585 (7)	4.5 (4)	C6F	0.3835 (11)	0.6103 (10)	0.1314 (7)	4.9 (4)
C1G	0.2929 (10)	0.0647 (9)	0.2245 (6)	3.8 (4)	C1G	0.1416 (10)	0.5395 (9)	0.2766 (7)	3.8 (4)
C2G	0.3768 (11)	0.0674 (10)	0.2111 (7)	4.8 (4)	C2G	0.0620 (11)	0.5193 (11)	0.2995 (7)	5.0 (4)
C3G	0.4313 (12)	0.0741 (11)	0.2510 (8)	5.7 (5)	C3G	−0.0029 (12)	0.5307 (11)	0.2604 (8)	5.6 (5)
C4G	0.3955 (12)	0.0787 (11)	0.3029 (8)	5.5 (4)	C4G	0.0149 (11)	0.5564 (11)	0.2035 (8)	5.2 (4)
C5G	0.3124 (12)	0.0835 (11)	0.3161 (8)	5.3 (4)	C5G	0.0934 (13)	0.5742 (12)	0.1810 (8)	6.2 (5)
C6G	0.2620 (11)	0.0728 (10)	0.2778 (7)	4.8 (4)	C6G	0.1567 (11)	0.5662 (11)	0.2188 (7)	5.0 (4)
C1H	0.2997 (10)	−0.0098 (9)	0.1310 (7)	3.9 (4)	C1H	0.1599 (10)	0.5861 (9)	0.3776 (7)	3.8 (4)
C2H	0.3001 (11)	−0.0971 (10)	0.1416 (7)	4.7 (4)	C2H	0.1080 (11)	0.5478 (10)	0.4180 (7)	4.8 (4)
C3H	0.3631 (13)	−0.1487 (12)	0.1099 (8)	6.1 (5)	C3H	0.0544 (12)	0.5958 (12)	0.4547 (8)	6.0 (5)
C4H	0.4180 (13)	−0.1115 (12)	0.0722 (9)	6.6 (5)	C4H	0.0584 (14)	0.6817 (13)	0.4490 (9)	7.4 (6)
C5H	0.4201 (13)	−0.0264 (12)	0.0616 (8)	6.2 (5)	C5H	0.1110 (12)	0.7195 (12)	0.4093 (8)	6.0 (5)
C6H	0.3570 (12)	0.0271 (11)	0.0906 (8)	5.4 (4)	C6H	0.1629 (10)	0.6712 (10)	0.3716 (7)	4.2 (4)

[a] The atom names for dications A and B are the same for chemically equivalent atoms. [b] Anisotropic thermal parameters are included as supplementary material.

Table IV. Selected Distances and Angles in the Dication $[Rh_2(CO)_2(PNP)_2]^{2+}$ (1)[a]

		Distances (Å)			
Rh-Rh′	3.054 (1)	P1-C7	1.868 (5)	C7-C8	1.523 (7)
Rh-P1	2.271 (1)	P1-C1A	1.810 (6)	N-C8	1.353 (7)
Rh-P2	2.358 (1)	P1-C1B	1.804 (6)	N-C10	1.347 (7)
Rh-N	2.187 (5)	P2-C7′	1.870 (5)	C10-C11	1.367 (8)
Rh-C	1.819 (6)	P2-C1C	1.841 (6)	C11-C12	1.371 (8)
C-O	1.137 (7)	P2-C1D	1.825 (6)	C12-C13	1.373 (8)
				C8-C13	1.383 (7)
		Angles (deg)			
P1-Rh-P2	176.70 (6)	Rh-P1-C7	99.1 (2)	P1-C7-P2′	112.4 (3)
P1-Rh-N	77.2 (1)	Rh-P2-C7′	111.3 (2)	P1-C7-C8	101.7 (4)
P1-Rh-C	92.2 (2)	Rh-P1-C1A	124.5 (2)	C7-C8-N	117.1 (5)
C-Rh-N	167.8 (2)	Rh-P1-C1B	112.2 (2)	C7-C8-C13	120.5 (5)
Rh-C-O	177.5 (6)	Rh-P2-C1C	122.3 (2)	N-C10-C11	123.6 (6)
Rh′-Rh-P1	93.7 (1)	Rh-P2-C1D	112.4 (2)	C10-C11-C12	119.1 (6)
Rh′-Rh-P2	85.8 (1)	Rh-N-C8	118.9 (3)	C11-C12-C13	118.9 (6)
Rh′-Rh-C	104.4 (1)	Rh-N-C10	123.5 (3)	C8-C13-C12	119.3 (6)
Rh′-Rh-N	82.5 (1)	C8-N-C10	116.8 (4)	C1A-P1-C1B	104.6 (3)
C7-P1-C1A	110.6 (2)	P2′-C7-C8	111.9 (4)	C1C-P2-C1D	98.0 (3)
C7-P1-C1B	104.2 (3)	C7′-P2-C1C	104.5 (3)	C7′-P2-C1D	106.7 (3)
P2-Rh-N	99.5 (2)	P2-Rh-C	91.1 (2)		

[a] Atoms with primes are related to their unprimed counterparts by crystallographic C_2 symmetry: $x, y, z \rightarrow -x, y, {}^1/_2 - z$.

analogue of **1** to form complex **2**, although it is not obvious which CO ligand has been added. In complex **2** the Ir–N separations are long (2.32 (2) Å), although still bonding, and ν(py CN) = 1596 cm^{-1}. In the IR spectrum (KBr disk) terminal and bridging CO stretching vibrations are apparent (ν(CO) = 1984, 1964, and 1803 cm^{-1}) and ν(py CN) = 1595 cm^{-1}. In CH_2Cl_2 solution, however, evidence for isomers with unbound N exists (ν(py CN) = 1596, 1586 cm^{-1}). The $^{31}P\{^1H\}$ NMR spectrum of **2** consists of a complex symmetric pattern cenetered at δ 28.1, which is best described as an approximate quartet of triplets (spectrum included as supplementary material[20]). The peaks in this spectrum have not been analyzed.

Attempts to prepare the rhodium analogue of **2** by addition of CO to **1** have been unsuccessful, and this illustrates an important difference in the PNP chemistry of rhodium and iridium.

X-ray Structure Determinations. The structure of **$[Rh_2(CO)_2(PNP)_2](PF_6)_2 \cdot C_3H_6O$ (1)** consists of discrete dications, anions, and acetone solvate molecules. There are no unusually short contacts between these species. Figure 1 shows an ORTEP drawing of the molecular structure of the dication including a labeling scheme. Selected distances and angles within the dication are presented in Table IV. A crystallographic twofold axis (C_2) passes through the midpoint of the Rh–Rh′ vector and relates the primed to the unprimed atoms in Figure 1. The dication is a bimetallic diphosphine-bridged molecule of the face-to-face variety. The coordination core around the Rh atom is approximately planar and consists of trans phosphorus atoms (P1–Rh–P2 = 176.70 (6)°), a CO group, and a N atom from the pyridyl part of the PNP ligand. The maximum deviation from the weighted least-squares plane that contains P1, P2, C, and N is 0.12 Å for C. The Rh atom is displaced 0.01 Å from this plane. The pyridyl N atom is bound to Rh (Rh–N = 2.187 (5) Å) and is approximately trans to the carbonyl C atom (N–Rh–C = 167.8 (2)°). The PNP ligand is therefore tridentate, forming a diphosphine bridge between the two Rh atoms and a P–N five-membered chelate ring to one Rh atom. The overall stereochemistry is cis with the CO groups and the pyridyl groups on the same side of the binuclear structure, respectively.

The chelate "bite" angle (P1–Rh–N = 77.2 (1)°) is similar to the value (75.9°) found in $[Rh(nbd)(PNP)]BF_4$,[15] but the Rh–N bond distance in **1** is somewhat longer (2.187 (5) vs. 2.148 (5) Å, respectively). In $[Rh(nbd)(PNP)]^+$ the PNP ligand is tridentate to one Rh atom.[15] The two Rh–P distances in **1** are significantly different (Rh–P1 = 2.271 (1) Å and Rh–P2 = 2.358 (1) Å) with the shorter one forming part of the P–N chelate ring. In $[Rh(nbd)(PNP)]BF_4$, the Rh–P distance is considerably longer (2.407 (1) Å), and this results from the considerable ring strain imposed by the unusual tridentate chelate nature of PNP in this complex.[15] The average Rh–P distance in **1** (2.315 (1) Å) is similar to values found in dppm-bridged binuclear complexes of Rh(I), which range from 2.30 to 2.34 Å;[3,4] however, the individual distances fall considerably outside of this range. The parameters involving the carbonyl ligands are not unusual, being typical for Rh(I) phosphino complexes.

The Rh–P vectors on each metal are significantly staggered when viewed down the Rh–Rh′ axis, as is shown by the P1–Rh–Rh′–P2′ torsion angle of 16.9°. This degree of twisting is rather large for dppm-bridged binuclear complexes and may be compared with values of 2.2, 1.9, and 4.4° for $[Rh_2Cl_2(CO)_2(dppm)_2]$,[3] $[Rh_2(\mu\text{-}Cl)(CO)_2(dppm)_2]BF_4$,[5] and $[Rh_2(\mu\text{-}CO)(\mu\text{-}Cl)(CO)_2(dppm)_2]BPh_4$,[6] respectively. While most structures of this type exhibit nearly eclipsed phosphine conformations, there are several that are significantly twisted. Torsion angles of 20.2 and 39° have been found for $[Rh_2(\mu\text{-}S)(CO)_2(dppm)_2]$[4] and $[Pd_2Cl_2(dppm)_2]$,[7] respectively. The twisting observed in **1** results from repulsion between the pyridyl rings. If the structure is twisted so that the Rh–P vectors are eclipsed, the shortest C···C contact between the pyridyl rings becomes less than 2 Å and therefore the eclipsed conformation is precluded.

The pyridyl ring is planar within experimental error and makes a dihedral angle of 30.9° with the square plane of the coordination core. The Rh atom is displaced 0.35 Å from the least-squares plane of the pyridyl ring in contrast to the case for $[Rh(nbd)(PNP)]BF_4$,[15] where there is no displacement observed. The dihedral angle between the square planes of the Rh and Rh′ coordination cores is 21.5° and shows that these planes are skewed such that the pyridyl nitrogen atoms are folded in toward the bridging sites between the metal centers. Thus, the nonbonded distances between N and N′, P1 and P2′, Rh and Rh′, C and C′ are 2.906 (8), 3.106 (3), 3.054 (1), 4.007 (8) Å, respectively. The square planes of the coordination cores are not perpendicular to the Rh–Rh′ vector but are inclined to it by ca. 80°. A similar twist of the Rh square planes was also observed in $[Rh_2Cl_2(CO)_2(dppm)_2]^+$ and appears to result from repulsions between the carbonyl group and the phenyl rings.

The Rh···Rh separation of 3.054 (1) Å is consistent with no formal metal–metal bond but is significantly shorter than

Table V. Selected Distances and Angles in the Dication $[Rh_2(\mu\text{-}CO)(CO)_2(PNP)_2]^{2+}$ (**2**)

Distances (Å)[a]					
Ir1-Ir2	2.815 (1)	Ir1-C12	2.02 (1)	P4-C24	1.86 (1)
Ir1-P1	2.319 (5)	Ir2-N24	2.32 (1)	C13-C13A	1.52 (2)
Ir1-P2	2.348 (5)	Ir2-C2	1.82 (2)	C24-C24A	1.51 (2)
Ir2-P3	2.355 (5)	Ir2-C12	2.01 (1)	C13A-N13	1.35 (2)
Ir2-P4	2.325 (5)	P1-C13	1.88 (1)	C24A-N24	1.35 (2)
Ir1-N13	2.32 (1)	P2-C24	1.87 (1)	C1-O1	1.18 (2)
Ir1-C1	1.82 (1)	P3-C13	1.86 (1)	C2-O2	1.16 (2)
				C12-O12	1.20 (2)

Angles (deg)[a]					
P1-Ir1-P2	172.0 (2)	N13-Ir1-C1	120 (1)	Ir1-Ir2-C2	153.3 (6)
P3-Ir2-P4	171.3 (2)	N13-Ir1-C12	128 (1)	Ir2-Ir1-C1	155.1 (6)
P1-Ir1-N13	73.3 (4)	C1-Ir1-C12	111 (1)	Ir1-P1-C13	100.0 (7)
P4-Ir2-N24	73.4 (5)	N24-Ir2-C2	122 (1)	Ir2-P3-C13	113.0 (7)
P1-Ir1-C1	89.8 (6)	N24-Ir2-C12	128 (1)	Ir1-P2-C24	113.0 (7)
P2-Ir1-C1	88.8 (6)	C2-Ir2-C12	109 (1)	Ir2-P4-C24	99.7 (6)
P3-Ir2-C2	88.7 (6)	Ir1-C12-Ir2	89 (1)	Ir1-N13-C13A	117 (1)
P4-Ir2-C2	90.2 (6)	Ir1-C12-O12	136 (1)	Ir2-N24-C24A	118 (1)
P1-Ir1-C12	91.6 (5)	Ir2-C12-O12	136 (1)	P1-C13-P3	110 (1)
P2-Ir1-C12	96.2 (6)	Ir1-C1-O1	175 (1)	P1-C13-C13A	101 (1)
P3-Ir2-C12	95.8 (6)	Ir2-C2-O2	176 (1)	P3-C13-C13A	111 (1)
P4-Ir2-C12	92.8 (5)	P2-C24-P4	110 (1)	N13-C13A-C13	120 (1)
P2-Ir1-N13	100.3 (4)	P2-C24-C24A	111 (1)	N24-C24A-C24	118 (1)
P3-Ir2-N24	100.0 (4)	P4-C24-C24A	102 (1)		

[a] The atom names correspond to those of dication A (Figure 2); however, since all chemically equivalent distances and angles for the two dications are within ±3 esd, the values reported are averages. The reported esd's are also averages.

the nonbonded Rh···Rh separations of 3.239 (:1), 3.152 (1), and 3.155 (4) Å observed in $[Rh_2Cl_2(CO)_2(dppm)_2]$,[3] $[Rh_2(\mu\text{-}Cl)(CO)_2(dppm)_2]BF_4$,[5] and $[Rh_2(\mu\text{-}S)(CO)_2(dppm)_2]$,[4] respectively. The Rh···Rh separation in **1** is the shortest thus far observed in any dppm-bridged binuclear complex of the face-to-face or non-carbonyl-bridged A-frame variety. The carbonyl-bridged A-frames have Rh···Rh separations more consistent with a Rh–Rh single bond: 2.757 (1), 2.732 (2), and 2.842 (1) Å for $[Rh_2(\mu\text{-}CO)Br_2(dppm)_2]$,[3a] $[Rh_2(\mu\text{-}H)(\mu\text{-}CO)(CO)_2(dppm)_2]^+$,[8] and $[Rh_2(\mu\text{-}CO)(\mu\text{-}Cl)(CO)_2(dppm)_2]^+$,[6] respectively. In **1** the Rh···Rh separation suggests significant, but nonbonding, metal–metal interaction and consistent with this the P···P intraligand separation (3.106 (3) Å) is slightly larger. The purple color of this complex respresents a considerable absorption shift toward the visible region compared to mononuclear square-planar rhodium complexes, which are usually yellow or orange. Similar shifts observed in the visible spectra of binuclear rhodium complexes have been explained as proximity-shifted M–L charge-transfer transitions.[21]

The structure of $[Ir_2(\mu\text{-}CO)(CO)_2(PNP)_2](BF_4)_2$ (**2**) consists of discrete dications and anions with no unusually short contacts between these ions. Figure 2 shows an ORTEP drawing of the molecular structure of dication A. The crystal structure contains two independent dications, A and B, in the asymmetric unit, but since there are no important differences between the two dications and all chemically equivalent distances and angles are within ±3 esd, the figures show only the A dication. The distances and angles that are listed in Table V and quoted in the text are averages for the two independent dications. Positional and thermal parameters are reported for both dications (Table III and supplementary material[20]), and the labeling scheme for dication B is identical with that of A.

The dication of **2** is a bimetallic diphosphine-bridged molecule with trans phosphines, a bridging CO ligand, and two terminal CO ligands. The structure is most similar to that of the double A-frame type C but with nonbridging pyridyl nitrogen atoms occupying the Y coordination positions of each iridium. An X-ray analysis has not been previously carried out on this structural type; however, similar structures have been proposed for $[Ir_2(\mu\text{-}CO)(CO)_3Cl(dpam)_2]^+$ and $[Rh_2(\mu\text{-}CO)(t\text{-}BuNC)_4(dppm)_2]^{2+}$, where dpam is the arsenic analogue of dppm.[9] The PNP ligands are tridentate and are disposed in a fashion similar to that of **1**. The coordination core of each Ir atom is approximately trigonal bipyramidal if the Ir–Ir interaction is ignored. The axial phosphorus atoms are approximately trans (average P–Ir–P 171.7 (2)°) and are essentially normal to the equatorial N,C,C planes. The atoms within the equatorial planes are approximately trigonal (average L_{eq}–Ir–L_{eq} angle 119.7°), and the Ir atoms are displaced 0.17 and 0.19 Å, respectively, for Ir1 and Ir2 from these equatorial N,C,C planes. The major distortion from trigonal-bipyramidal geometry is the less than 90° "bite" angle for the five-membered P–N chelate rings of the PNP ligands. These "bite" angles are 73.3 (4) and 73.4 (5)° around Ir1 and Ir2, respectively, and are smaller than the 77.2 (1)° value found in **1**. The smaller value in **2** results from the much longer Ir–PN ligand distances (Ir–P = 2.319 (5) and 2.325 (5) Å, Ir–N = 2.32 (1) and 2.32 (1) Å) in this compound compared with the analogous Rh–ligand distances in **1** (2.271 (1) and 2.187 (5) Å, respectively). The lengthening of these distances in **2** is due in part to increased crowding within the Ir coordination core compared with that of **1**.

The Ir–P bond lengths (average 2.337 (5) Å) are similar to those observed in $[Ir_2(\mu\text{-}S)(\mu\text{-}CO)(CO)_2(dppm)_2]$ (average 2.321 (3) Å)[10] and agree with those reported for other iridium phosphine complexes.[22,23] Similarly, the Ir–C distances for both terminal (1.82 (2) Å) and bridging carbonyls (2.02 (1) Å) correspond to reported values.[24,25] The Ir–N distances (2.32 (2) Å) are very long compared with values found in other Ir(I) complexes (2.180 (5) Å for $IrCl(CO)[(Ph_2P\text{-}o\text{-}C_6H_4)(Me_2N)]$[25]) and indicate very weak coordination. Indeed, the Ir–N distances are similar to the Ir–P distances. The weakness of this bond is presumably due to steric repulsion between the pyridyl group and the other ligands.

The Ir–P vectors on each metal are significantly staggered when viewed down the Ir–Ir axis. This twisting is very similar to that observed in **1** and seems to be a property of PNP-

---

[21] Balch, A. L.; Tulyathan, B. *Inorg. Chem.* **1977**, *16*, 2840.

[22] Hodgson, D. J.; Ibers, J. A. *Inorg. Chem.* **1969**, *8*, 1232.

[23] Brock, C. P.; Ibers, J. A. *Inorg. Chem.* **1972**, *11*, 2812.

[24] Pierpont, C. G.; Stuntz, G. F.; Shapley, J. R. *J. Am. Chem. Soc.* **1978**, *100*, 616.

[25] Roundhill, D. M.; Bechtold, R. A.; Roundhill, S. G. N. *Inorg. Chem.* **1980**, *19*, 284.

bridged binuclear complexes of this type. The P1–Ir1–Ir2–P3 and P2–Ir1–Ir2–P4 torsion angles are 14.9 and 14.4°, respectively, and are similar to the 16.9° value observed in **1**. The trigonal planes about Ir1 and Ir2 are also skewed (dihedral angle between the trigonal planes 30.9°) due to this twisting. As in **1** this twisting is due to the close cis proximity of the pyridyl rings. The pyridyl rings are each planar within experimental error, and the Ir1 and Ir2 atoms are displaced 0.18 and 0.15 Å, respectively, from these least-squares planes. The dihedral angle between the two pyridyl planes is 14.4°, and this may be compared to the analogous angle of 19.7° in compound **1**.

The Ir–Ir separation (2.815 (1) Å) is slightly longer than the mean distance of ca. 2.76 Å[24,26,27] found in polynuclear iridium cluster compounds and is consistent with an Ir–Ir single bond. The Ir–Ir single bond gives an 18e configuration to each of the two metal centers. The compression along the Ir–Ir internuclear axis is evident in a shorter separation between the metals than between adjacent PNP phosphorus atoms (P1···P3 = 3.054 (8) Å, P2···P4 = 3.049 (8) Å). Also, the acute Ir1–C12–Ir2 angle of 89 (1)° compares well with other values reported for carbonyls bridging Ir–Ir and Rh–Rh bonds.[6,10]

Reaction Chemistry of Rh and Ir PNP Complexes. The reaction of $[Rh_2(CO)_2(PNP)_2]^{2+}$ (**1**) with Na_2S in methanol gives an immediate color change from purple to red. The product of this reaction is formulated as $[Rh_2(\mu\text{-}S)(CO)_2(PNP)_2]$ (**4**). The proposed structure of **4** is that of a sulfide-bridged A-frame of type B in which the N atoms of the PNP ligands are unbound. This structure is based on IR (ν(py CN) = 1582 cm^{-1}, ν(CO) = 1935 cm^{-1}) and $^{31}P\{^1H\}$ NMR ($CDCl_3$ solution), δ 30.3 symmetric multiplet with two principal lines separated by ~139 Hz) evidence. The ν(py CN) stretching frequency is very similar to that of the free PNP ligand, and the ^{31}P NMR spectrum is typical of the complex pattern observed for dppm-bridged A-frames of rhodium.[2,9] A figure of this spectrum is included as supplementary material.[20]

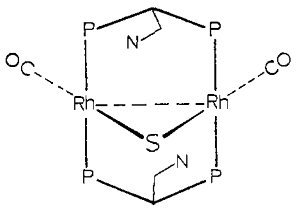

4

The reaction of a purple, dry acetone solution of **1** with 2 equiv of chloride gives the yellow monomeric PN-bonded complex [Rh(CO)(Cl)(PNP)] (**5**). The structure of this complex was deduced from its $^{31}P\{^1H\}$ NMR (acetone solution) and IR (KBr disk) spectra [ν(CO) = 1990 cm^{-1}, ν(py CN) = 1601 cm^{-1}; δ_1 = 69.1 (d of d, J_{Rh-P} = 168 and $J_{P-P'}$ = 108 Hz (int = 1)), δ_2 = 0.35 (d, $J_{P-P'}$ = 108 Hz (int = 1))]. These data clearly show that the pyridyl nitrogen atom is bound and that one phosphorus atom is unbound. The unbound phosphorus atom resonates with a chemical shift in the region typical of free PNP ligand,[15] and Rh–P coupling is absent. The placement of CO trans to N in **5** is considered reasonable but is by no means uniquely determined from the spectroscopic data. However, the similar iridium complex chlorocarbonyl(*o*-(diphenylphosphino)-*N*,*N*-dimethylaniline)iridium(I) has the same coordination core stereochemistry as is proposed for **5**.[25] In addition, the complex Rh(CO)(Cl)(PN), where PN = diphenylphosphino(2-pyridyl)methane, has also been shown to have the same stereochemistry.[28] The rapid formation of **5** represents a cleavage reaction of the PNP-bridged dimer in such a way that the PN chelate ring is preserved. The replacement of the bridging phosphorus atoms by chloride is a clean reaction since no intermediate compounds are observed by ^{31}P NMR during the slow addition of Cl^- to **1**. Only resonances due to **1** and **5** are apparent.

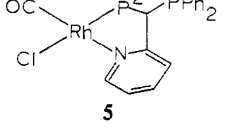

5

The yellow acetone solution of **5** is sensitive to moisture. Addition of water (only 5% by volume) results in an immediate color change to purple, and spectroscopic analysis shows that the parent complex **1** is quantitatively re-formed. The presence of the more polar, hydrogen-bonding solvent causes ionization of chloride and the re-formation of the dicationic binuclear complex. The addition of Na_2S to an acetone solution of **5** results in the formation of complex **4**.

The reaction of a green acetone solution of $[Ir_2(CO)_2(PNP)_2](BF_4)_2$ (**3**) with 1 equiv of a nucleophile X, such as Cl^- or I^-, gives the yellow dimeric complex $[Ir_2(CO)_2(X)(PNP)_2](BF_4)$ (**6**). The structure of this complex was deduced from its IR (Experimental Section) and $^{31}P\{^1H\}$ NMR spectra. The ^{31}P NMR spectrum of **6** (X = I) recorded with CH_2Cl_2 as solvent shows four well-separated multiplets, each a doublet of doublets of doublets, centered at δ = 8.83, 18.5, 31.6, and 39.2. A trace of the spectrum is included as supplementary material.[20] These data are consistent with a structure that contains one bound and one unbound pyridyl N atom and four nonequivalent phosphorus atoms as shown in the drawing of **6**. The trans stereochemistry of the bridging phosphorus atoms is also confirmed by the magnitude of the P–P coupling constants (J_{trans} = 347, 324, 347, and 324 Hz, J_{cis} = 78, 78, 57, and 57 Hz, and J_{cis} = 21, 15, 15, and 21 Hz, respectively, for the four multiplets in order of increasing δ). The large P–P coupling is only consistent with the trans-phosphorus stereochemistry. The spectroscopic results for the X = Cl complex are qualitatively similar. Addition of a second equivalent of nucleophile to **6** does not result in replacement of the second pyridyl N atom.

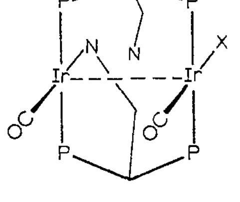

6

These reactions illustrate important differences in the PNP chemistry of Rh and Ir and show good prospects for future research. Work under current study includes the reactions of complexes **1**–**3** with small molecules such as H_2, CO_2, olefins, and H_2S. These studies also include an investigation into the catalytic properties of Rh and Ir PNP complexes.

Acknowledgment. Support of this research through a grant from the National Science Foundation is gratefully acknowledged (NSF Grant No. CHE 81-08490). We also thank the NSF for partial support for our X-ray diffraction and structure-solving equipment (NSF Grant No. CHE 77-28505). The Johnson-Matthey Co. is gratefully acknowledged for generous loans of rhodium and iridium salts. M.P.A. is a participant in the U.S. Air Force Institute of Technology Graduate School Program. B.M.M. acknowledges the Graduate School of Creighton University for a Summer Faculty Research Fellowship.

---

(26) Shapley, J. R.; Stuntz, G. F.; Churchill, M. R.; Hutchinson, J. P. *J. Am. Chem. Soc.* **1979**, *101*, 7425.

(27) Wang, H. H.; Pignolet, L. H. *Inorg. Chem.* **1980**, *19*, 1470.

(28) Anderson, M. P.; Boyle, P.; Pignolet, L. H., results to be submitted for publication.

Registry No. **1**, 86992-66-7; **2**, 86943-70-6; **3**, 86943-72-8; **4**, 86943-73-9; **5**, 86943-74-0; **6**, 86943-76-2; [Rh(nbd)(PNP)]PF_6, 86953-28-8; [Ir(cod)(PNP)]BF_4, 86953-30-2; $[Ir(cod)Cl]_2$, 12112-67-3.

Supplementary Material Available: Tables of general temperature factor expressions, calculated hydrogen atom positional parameters, and calculated and observed structure factor amplitudes for **1** and **2**, figures of ^{31}P NMR spectra for compounds **2**, **3**, **4**, and **6**, and stereoviews of **1** and **2** (62 pages). Ordering information is given on any current masthead page.

Contribution from the W. R. Kenan, Jr. Laboratory, Department of Chemistry,
The University of North Carolina, Chapel Hill, North Carolina 27514

Chemical, Spectral, and Structural Features of $Mo(RC{\equiv}CR)_2(S_2CNC_4H_4)_2$ Complexes Containing the Electronically Unique Pyrrole-*N*-carbodithioate Ligand

RICHARD S. HERRICK, SHARON J. NIETER BURGMAYER, and JOSEPH L. TEMPLETON*

Received December 21, 1982

Syntheses of a series of bis(alkyne)bis(pyrrole-*N*-carbodithioato)molybdenum(II) complexes, including the unsubstituted acetylene derivative $Mo(HC_2H)_2(S_2CNC_4H_4)_2$, are reported. The molecular structure of the 2-butyne adduct, $Mo(MeC_2Me)_2(S_2CNC_4H_4)_2$, has been determined by a single-crystal X-ray diffraction study. The crystals were found to be monoclinic of space group $P2_1/n$ with $a = 12.372$ (4) Å, $b = 12.145$ (3) Å, $c = 14.184$ (3) Å, and $\beta = 101.50$ (2)°. The unit cell contains one independent molecule per asymmetric unit; the structure was refined to $R = 0.056$ and $R_w = 0.041$ with use of 1470 reflections with $I > 3\sigma(I)$. The molecular geometry can be described as a distorted octahedron with two cis-parallel alkynes and two bidentate carbodithioates in the coordination sphere. The pyrrole-*N*-carbodithioate ligands are essentially planar with a C–N distance of 1.37 Å (average) in the $S_2C\text{–}NC_4H_4$ unit. The ring distances within the NC_4H_4 moiety are compared to those of free pyrrole and cyclopentadiene to address the question of aromaticity in this fragment. Dynamic NMR studies revealed two independent fluxional processes in $Mo(MeC_2Me)_2(S_2CNC_4H_4)_2$. The lower energy process ($\Delta G^* = 10.7$ kcal/mol) is believed to reflect rotation around the C–N bond of the chelating ligands while the higher energy molecular rearrangement (13.7 kcal/mol) is believed to correspond to rotation of the alkyne ligands around the molybdenum–alkyne bond axis. Both the crystallographic and DNMR results reflect the pyrrole nitrogen's reluctance to provide π-electron density to the CS_2 fragment. The decreased electron donor ability of the pyrrole-*N*-carbodithioate ligand relative to that of alkyl analogues is chemically evident in the lability of the carbonyl ligand in $Mo(CO)(RC_2R)(S_2CNC_4H_4)_2$, which greatly enhances the rate of formation of the bis(alkyne) products. The chemical, spectroscopic, and structural properties of these complexes can be rationalized in terms of accepted valence bond descriptions of carbodithioate ligands.

Introduction

The chemistry of low-oxidation-state, formally electron-deficient d^4 transition-metal monomers containing both π-acid and π-base ligands has matured substantially.[1] A useful model of the electronic structure of these compounds[2] has been distilled from the spectroscopic,[3–6] structural,[1,7,8] theoretical,[9] electrochemical[1c,10] and mechanistic[11] results accumulated for these complexes.

A significant subclass of six-coordinate d^4 monomers is the set of bis(dithiocarbamato) derivatives of the type $M(X)(Y)(S_2CNR_2)_2$ (M = Mo, W; X = Y = CO;[12] X = CO, Y = $R^1C_2R^2$;[7,13] X = O, Y = $R^1C_2R^2$;[4,8,14] X = Y = $R^1C_2R^2$[2,3,6]). The dithiocarbamate ligands serve to anchor these complexes by providing a variable degree of π-electron donation as evident in the chemistry[12] and structure[15] of $Mo(CO)_2(S_2CNR_2)_2$. Contributions from the three resonance forms (I–III) which

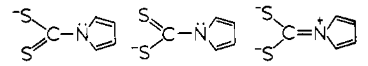

dominate metal–dithiocarbamate valence bond descriptions are relatively insensitive to minor variations of alkyl and aryl substituents on the nitrogen atom.[16] The pyrrole-*N*-carbodithioate ligand (pdtc) prepared by Kellner et al.[17] exhibits unusual bonding properties in homoleptic dithiocarbamate complexes. Bereman and his co-workers have substantiated the hypothesis that resonance form III is unfavorable for pdtc

---

(1) (a) Chisholm, M. H.; Huffman, J. C.; Kelly, R. L. *J. Am. Chem. Soc.* **1979**, *101*, 7615. (b) Churchill, M. R.; Wasserman, H. J. Holmes, S. J.; Schrock, R. R. *Organometallics* **1982**, *1*, 766. (c) Winston, P. B.; Nieter-Burgmayer, S. J.; Templeton, J. L. *Ibid.* **1983**, *2*, 167. (d) DeCian, A.; Cobin, J.; Schappacher, M.; Ricard, L.; Weiss, R. *J. Am. Chem. Soc.* **1981**, *103*, 1850. (e) Faller, J. W.; Murray, H. H. *J. Organomet. Chem.* **1979**, *172*, 171. (f) Davidson, J. L.; Green, M.; Stone, F. G. A.; Welch, A. J. *J. Chem. Soc., Dalton Trans.* **1976**, 738. (g) Watson, P. L.; Bergman, R. G. *J. Am. Chem. Soc.* **1980**, *102*, 2698.

(2) Templeton, J. L.; Winston, P. B.; Ward, B. C. *J. Am. Chem. Soc.* **1981**, *103*, 7713.

(3) McDonald, J. W.; Newton, W. E.; Creedy, C. T. C.; Corbin, J. L. *J. Organomet. Chem.* **1975**, *92*, C25.

(4) Templeton, J. L.; Ward, B. C.; Chen, G. J.-J.; McDonald, J. W.; Newton, W. E. *Inorg. Chem.* **1981**, *20*, 1248.

(5) Templeton, J. L.; Ward, B. C. *J. Am. Chem. Soc.* **1980**, *102*, 3288.

(6) Herrick, R. S.; Templeton, J. L. *Organometallics* **1982**, *1*, 842.

(7) Ricard, L.; Weiss, R.; Newton, W. E.; Chen, G. J.-J.; McDonald, J. W. *J. Am. Chem. Soc.* **1978**, *100*, 1318.

(8) Newton, W. E.; McDonald, J. W.; Corbin, J. L.; Ricard, L.; Weiss, R. *Inorg. Chem.* **1980**, *19*, 1997.

(9) Kubâček, P.; Hoffmann, R. *J. Am. Chem. Soc.* **1981**, *103*, 4320.

(10) Templeton, J. L.; Herrick, R. S.; Morrow, J. R. *Organometallics*, in press.

(11) Herrick, R. S.; Leazer, D. M.; Templeton, J. L. *Organometallics* **1983**, *2*, 834.

(12) (a) Colton, R.; Scollary, G. R.; Tomkins, I. B. *Aust. J. Chem.* **1968**, *21*, 15. (b) Templeton, J. L. *Adv. Chem. Ser.* **1979**, *No. 173*, 263. (c) Brooomhead, J. A.; Young, C. G. *Aust. J. Chem.* **1982**, *35*, 277.

(13) Ward, B. C.; Templeton, J. L. *J. Am. Chem. Soc.* **1980**, *102*, 1532.

(14) (a) Maatta, E. A.; Wentworth, R. A. D.; Newton, W. E.; McDonald, J. W.; Watt, G. D. *J. Am. Chem. Soc.* **1978**, *100*, 1320. (b) Maatta, E. A.; Wentworth, R. A. D. *Inorg. Chem.* **1979**, *18*, 524.

(15) Templeton, J. L.; Ward, B. C. *J. Am. Chem. Soc.* **1980**, *102*, 6568.

(16) Coucouvanis, D. *Prog. Inorg. Chem.* **1979**, *26*, 301.

(17) (a) Kellner, R.; Prokopowski, P.; Malissa, H. *Anal. Chim. Acta* **1974**, *68*, 401. (b) El A'mma, A. G.; Drago, R. S. *Inorg. Chem.* **1977**, *16*, 2975.

0020-1669/83/1322-3275$01.50/0 © 1983 American Chemical Society